Spectral fluctuation and correlation structure of δ_n statistics in the spectra of interacting trapped bosons

Kamalika Roy,[1] Barnali Chakrabarti,[2] and V. K. B Kota[3]
[1]*Department of Physics, Lady Brabourne College, P1/2 Suhrawardi Avenue, Kolkata 700017, India*
[2]*Department of Physics, University of Kalyani, Kalyani 741235, India*
[3]*Physical Research Laboratory, Navarangpura, Ahmedabad 380009, India*
(Received 16 January 2013; published 3 June 2013; corrected 12 March 2014)

It is a well-known fact that the statistical behaviors of level fluctuation and level correlation in the energy-level spectra are the most efficient tool to characterize quantum chaos in nonintegrable quantum systems. The system of interacting trapped bosons is a complex system where the low-lying energy levels are highly influenced by the level repulsion. In this case, interatomic interaction is a dominating fact with strong level correlation between distant levels. Here we numerically calculate the correlation function, number variance, and Dyson-Mehta least-square deviation for the low-lying levels for a few thousand interacting trapped bosons, and our data show good analogy with the Gaussian orthogonal ensemble (GOE) results with a signature of chaos. In the next part of our study, the energy spectrum of these low-lying levels is considered as a discrete signal and the fluctuation of the excitation energy is considered as discrete time series. Then we calculate numerically the height-height correlation function for different order of momentum. In our study logarithmic correlation structure is found instead of multiscaling structure, and we observe that spectral statistics are compatible with those of GOE.

DOI: 10.1103/PhysRevE.87.062101 PACS number(s): 05.30.Jp, 03.75.Hh, 05.45.Mt, 05.45.Tp

I. INTRODUCTION

The study of energy level fluctuations and level correlation functions is one of the most important tools for understanding of fluctuation measures in the spectra of complicated systems. The pioneering work of Bohigas [1] showed that the complex systems exhibit universal spectral fluctuation. It is well-established fact that the generic quantum systems are either integrable or chaotic depending on their spectral statistics. In the integrable systems the level clustering is one of the significant features, whereas in the chaotic systems level clustering is suppressed due to level repulsion. Strong level correlation in such systems is well described by the random matrix theory.

The n-level correlation function $R_n(E_1, E_2, \ldots, E_n)$ of an infinite stationary spectrum with unit average spacing determines all fluctuation measures. The spectral correlation crucially depends on the so-called two-point correlation function $R_2(E_1, E_2)$. Although the nearest neighbor spacing distribution is often used to describe level correlation and level repulsion; however, it depends on the n-level correlation function in a complicated way. The other popular quantity is the number variance Σ^2, which can be easily derived from the two-level correlation function and is widely used to describe level clustering. For a stationary spectrum we define the variable $n(L)$, which counts the number of levels contained in an interval of length L. The average of number statistics is $\langle n(L)\rangle = L$, and its variance $\Sigma^2(L)$ is a two-point measure and is given by

$$\Sigma^2(L) = \langle (n(E,L) - L)^2 \rangle. \tag{1}$$

It can be verified that for integrable systems $\Sigma^2(L) = L$, whereas for Gaussian ensembles $\Sigma^2(L)$ increases logarithmically for large L. Both $\Sigma^2(L)$ and R_2 have widely been used for the nuclear data ensemble [1–3]. The other frequently used quantity is the spectral rigidity or Δ_3 statistics, which is again based on the two-level correlation function [1–3]. It measures the size of fluctuations of the staircase function around a best fit straight line. Both Σ^2 and Δ_3 statistics are based on the two-point correlation function. Comparison between RMT predictions and numerical results for higher-order correlations may provide new information for complex systems.

Recently a different approach has been proposed to study the spectral fluctuation. Level fluctuation can be studied by the Fourier power spectrum where the energy spectrum is considered as a discrete signal while energy plays the role of time and the fluctuations of the excitation energy are considered as discrete time series. The appropriate statistical tool for the time series analysis is δ_n statistics. It is well-established fact that δ_n statistics exhibits a power law, and the chaotic quantum systems are characterized by $\frac{1}{f}$ noise, while the integrable quantum systems exhibit $\frac{1}{f^2}$ noise [4–7]. The correlation structure of δ_n statistics for chaotic systems has also been studied [8].

The statistical behavior and correlation properties of energy spectrum in complex atoms, atomic nuclei, quantum billiards, and chaotic complex quantum systems have been extensively studied [3,9–20]. The level fluctuation in complex systems is well described by the Gaussian orthogonal ensemble (GOE) of random matrices. However, very recently the noninteracting and weakly interacting many-bosons systems with an external confinement have drawn special attention [15–20]. Weakly interacting trapped bosons are especially interesting in the context of a Bose-Einstein condensation (BEC) and exhibits very complex energy spectrum [21,22]. Due to the presence of external confinement the energy spectrum shows a transition from a collective nature to a single-particle nature [23,24]. Apparently it appears that due to the presence of harmonic potential and weak interaction the system will exhibit the features of generic harmonic oscillator. However, from our earlier studies of dynamic and statistical properties, we have observed that the system of interacting trapped bosons is a highly complex system due to the interplay of two energy

scales [21,22]. The trap energy is characterized by $\hbar\omega$ (ω is the external trap frequency), and the interatomic interaction is characterized by Na_s (N is the number of bosons and a_s is the s-wave scattering length). In our earlier study [21,22] focus has been on a large set of energy levels, including both low- and high-level statistics, while in the present article the focus is on the lowest 100 levels. So the calculations presented here can be understood as a stringent test of what is just sketched in Refs. [21,22]: the fact that at low energies the system is chaotic. The universal hypothesis of Bohigas, Giannoni, and Schmit is also not followed by such a complex system. A highly unusual property of our model is that here the lowest energy levels are expected to behave statistically according to the random matrix theory predictions. This feature is in contrast to the standard lore of quantum chaos, which states that only highly excited (semiclassical) quantum energy levels reflect universal statistics inherited from the chaotic classical dynamics, whereas the low-lying excitations are system specific.

It is already observed both theoretically and experimentally that the low-lying levels are highly influenced by the interatomic interaction. These levels are highly correlated and we observe them to be close with the GOE. Thus the study of level repulsion, correlation function, and correlation structure of the δ_n statistics of such a realistic system especially for the low-lying levels may provide exciting information. In the past, for example, for the nuclear data ensemble, a realistic system, third and fourth order correlations in number statistics have been studied successfully [25]. The key motivation of our present work is to calculate the correlation properties using higher-order moments (up to order 10) of the power spectrum and get precise measures of level repulsion and long-range order in the system of interacting trapped bosons. The many-bosons system is solved by using a correlated two-body basis function, and a van der Waals potential is taken as the interatomic interaction. The use of a correlated basis function together with the realistic interatomic interaction will give the accurate results of level correlation and long-range order.

In Sec. II we present the many-body formalism to calculate the many-body effective potential and to compute the energy levels. Section III deals with several statistical tools in level correlation function, time series, correlation structure of δ_n statistics, etc., also with corresponding results. Section IV concludes the summary.

II. METHODOLOGY

For the purpose of the calculation of the energy levels of condensate we solve the Schrödinger equation using our newly adopted correlated potential harmonic expansion method (CPHEM), which has already been established as a very successful technique for the study of dilute BEC [26–28]. This method basically uses a truncated two-body basis set which keeps all possible two-body correlations. By considering a realistic interatomic interaction we go beyond the uncorrelated mean-field Gross-Pitaevskii (GP) theory [29,30]. We discuss our many-body method bringing out the salient features below.

For a system of $A = (N + 1)$ identical bosons interacting via two-body potential $V(\vec{r}_{ij}) = V(\vec{r}_i - \vec{r}_j)$, confined in an external harmonic potential of frequency ω, the time-independent quantum many-body Schrödinger equation looks like

$$\left[-\frac{\hbar^2}{2m}\sum_{i=1}^{A}\nabla_i^2 + \sum_{i=1}^{A} V_{\rm trap}(\vec{r}_i) + \sum_{i,j>i}^{A} V(\vec{r}_i - \vec{r}_j) - E \right] \times \Psi(\vec{r}_1,\ldots,\vec{r}_A) = 0, \tag{2}$$

where m is the mass of each boson, E is the energy of the condensate, $V_{\rm trap}(\vec{r}_i)$ is the external trapping potential and $V(\vec{r}_i - \vec{r}_j)$ is the two-body pair interaction. We use the standard Jacobi coordinates defined as $\vec{\zeta}_i = (\frac{2i}{i+1})^{\frac{1}{2}}[\vec{r}_{i+1} - \frac{1}{i}\sum_{j=1}^{i}\vec{r}_j]$, $i = 1,2,\ldots,N$, and the center of mass through $\vec{R} = \frac{1}{N+1}\sum_{i=1}^{N+1}\vec{r}_i$. Then the relative motion of the atoms is described in terms of N Jacobi vectors $(\vec{\zeta}_1,\ldots,\vec{\zeta}_N)$ as [26,31]

$$\left[-\frac{\hbar^2}{m}\sum_{i=1}^{N}\nabla_{\zeta_i}^2 + V_{\rm trap} + V(\vec{\zeta}_1,\ldots,\vec{\zeta}_N) - E \right] \times \Psi(\vec{\zeta}_1,\ldots,\vec{\zeta}_N) = 0. \tag{3}$$

The hyperspherical harmonic expansion method (HHEM) is an *ab initio* tool in many-body physics [31], where the expansion basis of the many-body wave function is the hyperspherical harmonics (HH). HHEM is a complete many-body approach that includes all the possible correlations. But its application to a typical BEC containing a few thousands to few millions of bosons seems to be an impossible task due to the large degeneracy of the HH basis, and consequently HHEM is restricted only to three-particle systems [31,32]. Thus for the spinless bosons, we decompose Ψ in two-body Faddeev components as

$$\Psi = \sum_{i,j>i}^{A}\Phi_{ij}(\vec{r}_{ij},r). \tag{4}$$

Here Φ_{ij} is a function of two-body separation $(\vec{r}_{ij})$, and the global hyperradius r is given by, $r^2 = r_{ij}^2 + \rho_{ij}^2$, while ρ_{ij} is defined as the hyperradius and ϕ as the hyperangle such that $r\sin\phi = \sqrt{\sum_{i=1}^{N}\zeta_i^2} = \rho_{ij}$ and $r_{ij} = r\cos\phi$. Φ_{ij} is symmetric under P_{ij} for bosons and satisfies the Schrödinger equation:

$$[T + V_{\rm trap} - E_R]\Phi_{ij} = -V(\vec{r}_{ij})\sum_{k,l>k}^{A}\phi_{kl}, \tag{5}$$

where $T = -\frac{\hbar^2}{m}\sum_{i=1}^{N}\nabla_{\zeta_i}^2$ is the total kinetic energy. Operating $\sum_{i,j\geq i}$ on both sides of Eq. (5), we get back the original Schrödinger equation. In this approach, we assume that when (ij) pair interacts, the rest of the bosons acts as inert spectators. Thus the total hyperangular momentum quantum number as well as the orbital angular momentum of the whole system is contributed by the interacting pair only. We expand (ij)-th Faddeev component, Φ_{ij}, in the complete set of Potential harmonics (PH) basis appropriate for the (ij) partition:

$$\Phi_{ij} = r^{-(\frac{3N-1}{2})}\sum_{K}\mathcal{P}_{2K+l}^{lm}(\Omega_N^{(ij)})u_K^l(r). \tag{6}$$

Ω_N^{ij} denotes the full set of hyperangles in the $3N$-dimensional space corresponding to the (ij)-th interacting pair, and

$\mathcal{P}^{lm}_{2K+l}(\Omega^{ij}_N)$ is called the PH basis having the analytic expression:

$$\mathcal{P}^{l,m}_{2K+l}\left(\Omega^{(ij)}_N\right) = Y_{lm}(\omega_{ij})\ {}^{(N)}P^{l,0}_{2K+l}(\phi)\mathcal{Y}_0(D-3); \quad D=3N, \tag{7}$$

where $Y_{lm}(\omega_{ij})$ is the spherical harmonics and $\omega_{ij}=(\vartheta,\varphi)$. The function ${}^{(N)}P^{l,0}_{2K+l}(\phi)$ is expressed in terms of Jacobi polynomials, and $\mathcal{Y}_0(3N-3)$ is the HH of order zero in the $(3N-3)$ dimensional space, spanned by $\{\vec{\zeta}_1,\ldots,\vec{\zeta}_{N-1}\}$ Jacobi vectors [31]. Thus the contribution to the grand orbital quantum number comes only from the interacting pair, and the $3N$ dimensional Schrödinger equation reduces effectively to a four-dimensional equation. The relevant set of quantum numbers are three: orbital l, azimuthal m, and grand orbital $2K+l$. K is the hyperangular momentum quantum number. The full set of quantum numbers are

$$l_1=l_2=\cdots=l_{N-1}=0, \quad l_N=l, \tag{8}$$

$$m_1=m_2=\cdots=m_{N-1}=0, \quad m_N=m, \tag{9}$$

$$n_2=n_3=\cdots=n_{N-1}=0, \quad n_N=K. \tag{10}$$

Taking the projection of Schrödinger equation on a particular PH, a set of coupled differential equations is obtained [26,28]:

$$\left[-\frac{\hbar^2}{m}\frac{d^2}{dr^2}+\frac{\hbar^2}{mr^2}\{\mathcal{L}(\mathcal{L}+1)+4K(K+\alpha+\beta+1)\}\right.$$
$$\left.-E+V_{\rm trap}(r)\right]U_{Kl}(r)+\sum_{K'}f_{Kl}V_{KK'}(r)f_{K'l}U_{K'l}(r)=0, \tag{11}$$

where $\mathcal{L}=l+\frac{3A-6}{2}$, $U_{Kl}=f_{Kl}u^l_K(r)$, $\alpha=\frac{3A-8}{2}$, and $\beta=l+1/2$. f_{Kl} is a constant and represents the overlap of the PH for interacting partition with the sum of PHs corresponding to all partitions [33]. The potential matrix element $V_{KK'}(r)$ is given by

$$V_{KK'}(r)=\int P^{lm^*}_{2K+l}(\Omega^{ij}_N)V(r_{ij})P^{lm}_{2K'+1}\left(\Omega^{ij}_N\right)d\Omega^{ij}_N\,. \tag{12}$$

We disregard the effect of the strong short-range correlation in the PH basis. In the experimental BEC, which is extremely diluted, the average interparticle separation is assumed to be much larger than the range of two-body interaction. For the present study we consider a few thousand ^{87}Rb atoms in the JILA trap [29,34]. Throughout our calculation we choose $a_{ho}=\sqrt{\frac{\hbar}{m\omega}}$ as the unit of length (oscillator unit), and energy is expressed in units of the oscillator energy ($\hbar\omega$). The van der Waals potential has been chosen as the interatomic potential with a hard core of radius r_c, *viz.*, $V(r_{ij})=\infty$ for $r_{ij}\leqslant r_c$ and $-\frac{C_6}{r^6_{ij}}$ for $r_{ij}>r_c$. The strength C_6 is taken as 6.4898×10^{-11} o.u. for ^{87}Rb atoms in the JILA experiment [29]. In the mean-field GP equation, as the energy of the interacting pair is extremely small, the two-body interaction is generally represented by the s-wave scattering length (a_s) only. A positive value of a_s gives a repulsive condensate, and a negative value of a_s gives an attractive condensate. It disregards the detailed structure. The presence of essential singularity as r tends to zero, for the attractive contact δ interaction makes the Hamiltonian unbound from below. So in our present calculation we use a realistic interatomic potential like a van der Waals potential, that is associated with an attractive $-\frac{1}{r^6_{ij}}$ tail at larger separation and a strong repulsion at short separation. The inclusion of detailed structure in the two-body potential with the short-range repulsion core needs to include an additional short-range correlation in the PH basis. Now a_s can be obtained by solving the zero-energy two-body Schrödinger equation for the wave function $\eta(r_{ij})$

$$-\frac{\hbar^2}{m}\frac{1}{r^2_{ij}}\frac{d}{dr_{ij}}\left[r^2_{ij}\frac{d\eta(r_{ij})}{dr_{ij}}\right]+V(r_{ij})\eta(r_{ij})=0, \tag{13}$$

and the correlation function quickly attains its asymptotic form $(1-\frac{a_s}{r_{ij}})$ for large r_{ij}. The short-range correlation function $\eta(r_{ij})$ is a good approximation of the short-range behavior of the Faddeev component. Replacing Eq. (5) by

$$\Phi_{ij}(\vec{r}_{ij},r)=r^{-(\frac{3N-1}{2})}\sum_K\mathcal{P}^{lm}_{2K+l}\left(\Omega^{ij}_N\right)u^l_K(r)\eta(r_{ij}), \tag{14}$$

and the correlated PH (CPH) basis becomes

$$\left[\mathcal{P}^{l,m}_{2K+l}\left(\Omega^{(ij)}_N\right)\right]_{\rm correlated}=\mathcal{P}^{l,m}_{2K+l}\left(\Omega^{(ij)}_N\right)\eta(r_{ij}). \tag{15}$$

The correlated potential matrix $V_{KK'}(r)$ is now given by

$$V_{KK'}(r)=\left(h^{\alpha\beta}_K h^{\alpha\beta}_{K'}\right)^{-\frac{1}{2}}\int_{-1}^{+1}\left\{P^{\alpha\beta}_K(z)V\left(r\sqrt{\frac{1+z}{2}}\right)\right.$$
$$\left.\times P^{\alpha\beta}_{K'}(z)\eta\left(r\sqrt{\frac{1+z}{2}}\right)W_l(z)\right\}dz. \tag{16}$$

Here $P^{\alpha\beta}_K(z)$ is the Jacobi polynomial with its norm $h^{\alpha\beta}_K$ and the weight function $W_l(z)$ [35]. The value of r_c is obtained subject to the requirement that the calculated a_{sc} has the expected value [36]. This is an improvement of the rate of convergence of the PH basis, and we call it a correlated potential harmonic expansion method (CPHEM).

It is to notify that the PH basis becomes nonorthogonal after the inclusion of $\eta(r_{ij})$, and that is why one should use the standard procedure for handling nonorthogonal basis. However, in the present calculation we have checked that $\eta(r_{ij})$ differs from a constant value only by small amount, and the overlap $\langle\mathcal{P}^{l,m}_{2K+l}(\Omega^{(ij)}_N)|\mathcal{P}^{l,m}_{2K+l}(\Omega^{(kl)}_N)\eta(r_{kl})\rangle$ is really very small. Thus we get back the Eq. (11) approximately when the correlated potential matrix is calculated by Eq. (16).

Finally the set of coupled differential equation [Eq. (13)] can be solved by the hyperspherical adiabatic approximation (HAA) [37]. It is assumed that the hyperadial motion is slow in comparison with the hyperangular motion. For the hyperangular motion for a fixed value of r, the potential matrix is diagonalized together with the hypercentrifugal term. The energy is thus obtained by solving the equation for the hyperradial motion [37] as

$$\left[-\frac{\hbar^2}{m}\frac{d^2}{dr^2}+\omega_0(r)-E_R\right]\zeta_0(r)=0 \tag{17}$$

subject to the appropriate boundary conditions on $\zeta_0(r)$, while E_R is the relative energy of the system, and the lowest eigenvalue ω_0 is the effective potential for the hyperradial motion. The function $\zeta_0(r)$ is the collective wave function of

the condensate in the hyperradial space. Thus in our many-body picture the collective motion of the entire condensate is characterized by the effective potential.

The excited states in this potential are the states with the lth surface mode and nth radial excitation, which are denoted by E_{nl}. Thus $n = 0$ and $l = 0$ correspond to the ground state, and for $l \neq 0$, we get the surface modes. To calculate the higher levels with $l \neq 0$, as a large inaccuracy is involved in the calculation of off-diagonal potential matrix, numerical computation becomes very slow. However, the main contribution to the potential matrix comes from the diagonal hypercentrifugal term, and the off-diagonal matrix element for $l > 0$ is ignored. Thus we get the effective potential $\omega_l(r)$ in the hyperradial space for $l \neq 0$. The energy of the lowest modes is in close agreement with the other calculations [23,24,38,39].

It is to be noted that in the experimental realization of BEC in trapped Bose gases there is intensive study of the excitations in these systems [23,24]. Measurements of the lowest modes are especially important when several interesting features are explored in the dynamical behavior of trapped gases [23,24]. The nature of collective excitations of trapped gas is quite different from superfluid ^{4}He. Although the Bose gas is extremely dilute it is experimentally observed that the interatomic interaction has an important role and the low-energy excitations are of collective nature, whereas the harmonic confinement makes the high-lying levels of single-particle nature [21–24]. Thus in our present work we mainly consider various correlation properties and fluctuation measures for low-lying levels (lowest 100 levels), which are of collective nature.

III. STATISTICAL TOOLS AND RESULTS

To characterize spectral fluctuation and correlation function we unfold the energy level sequence using a seventh-order polynomial. The unfolding procedure removes the smooth part of the energy spectrum and maps the energy levels to another with the mean level density equal to 1. As stated in the Introduction, the correlation properties of the energy level sequence $\{E_i\}$ are characterized by the set of n-level correlation function $R_n(E_1, E_2, \ldots, E_n)$ [1–3] as

$$R_n(E_1,\ldots,E_n) = \frac{N!}{(N-n)!}\int P_N(E_1,\ldots,E_n)dE_{n+1}\ldots dE_N, \tag{18}$$

where $(E_1, \ldots, E_n) \equiv \{E_i\}$ denotes the positions of n points with average density unity. $P_N(E_1, \ldots, E_N)dE_1 \ldots dE_N$ measures the probability regardless of labeling of having one point at E_1, another at E_2, and so on. Thus the n-level correlation function is the probability density of observing a level at each of the n points $E_1, \ldots, E_n$ irrespective of the position of the other levels. Whereas the two-level correlation function $R_2(E_1, E_2)$ measures the probability density to find two eigenenergies E_1 and E_2 irrespective of the position of other eigenenergies.

In Fig. 1 we display our numerically calculated results of R_2 as a function of L for the lowest 100 levels and 5000 bosons in the trap. Numerical results are also compared with the analytic

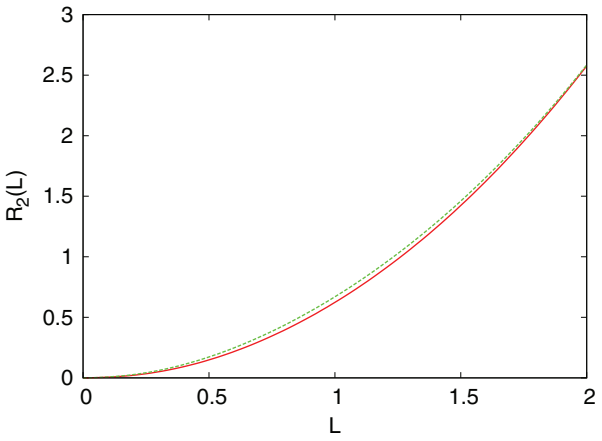

FIG. 1. (Color online) The plot of $R_2(L)$ against L for $N = 5000$ numbers of interacting trapped bosons and lowest 100 levels. The green dotted line represents the analytic results using Eq. (19), and the red solid line represents numerical results.

results given by

$$R_2(L) = \alpha L^2 + \beta L^3. \tag{19}$$

The calculated results are in good agreement with GOE results, which confirms the high correlation in the energy levels. At $L = 0$, our calculated $R_2(L)$ is zero, which is indeed necessary for level repulsion. Next to quantify the level repulsion at small distances, we perform a nonlinear fit to Eq. (19), and calculated values of α and β are presented in Table I.

Next, to calculate the number variance, i.e., Σ^2 statistics, we consider the number $n(E,L)$ of eigenvalues in length interval L, centered at the energy E. $n(E,L)$ is obtained from the density of states as

$$n(E,L) = \int_{E-\frac{L}{2}}^{E+\frac{L}{2}} \rho(E)\,dE. \tag{20}$$

The ensemble average of $n(E,L)$ becomes independent of E and $\langle n(E,L)\rangle = L$. Then for the unit mean level density energy sequence we define the variance of the number of eigenvalues as by Eq. (1). Now for uncorrelated energy eigen values, $\Sigma^2(L) = L$, whereas for a Gaussian ensemble with level repulsion $\Sigma^2(L)$ increases logarithmically. Our numerically calculated Σ^2 for lowest 100 levels with 5000 bosons in the external trap is presented in Fig. 2. For comparison with the analytic results we also plot Eq. (21) in the same figure for

TABLE I. Values of α and β as per Eq. (19) as well as the values of a, b, and c as per Eq. (21) in the range $1 \leqslant L \leqslant 10$. GOE values are also given [25] for the sake of comparison.

Coefficients	Numerical	GOE
α	0.01	0
β	0.45	0.54 ± 0.1
a	-0.005	0 ± 0.005
b	0.04	0.1 ± 0.02
c	0.44	0.44 ± 0.02

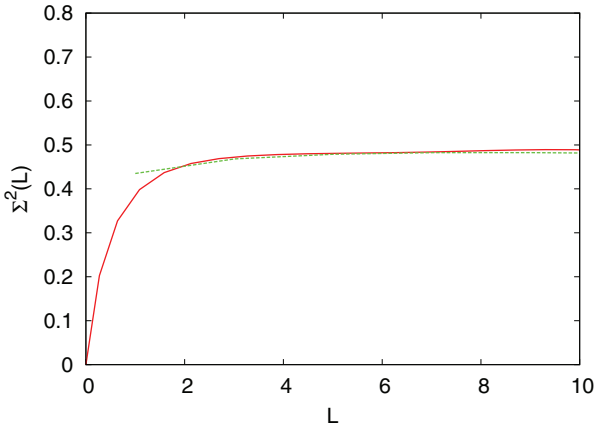

FIG. 2. (Color online) Plot of the variance $\Sigma^2(L)$ against L for $N = 5000$ numbers of interacting trapped bosons and for the lowest 100 levels. The red solid line represents results of numerical calculations, and the green dotted line represents the analytic Eq. (21) with a, b, and c given in Table I. The green curve stops at $L = 1$ as given by Eq. (21).

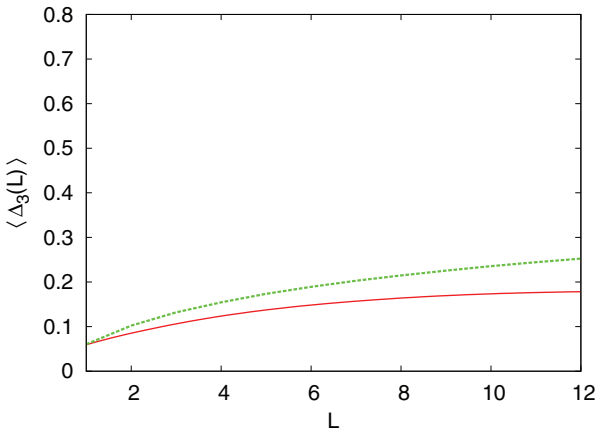

FIG. 3. (Color online) Red line is the plot of $\Delta_3(L)$ against L calculated for $N = 5000$ numbers of interacting trapped bosons and lowest 100 levels. The green dotted line gives GOE result.

larger L values with a, b, and c chosen from Table I. Nice agreement with the GOE distribution is found for larger L. Σ^2 measures large correlations between distant levels and determines long-range order. Next, to quantify it we fit our numerical results with the three-parameter expression of Σ^2 as

$$\Sigma^2(L) = a\ L + b\ \ln\ L + c \qquad (L \geqslant 1). \tag{21}$$

For long-range order $a = 0$, the value of b provides a measure of long-range order, smaller value of b signifies that the spectrum is rigid, whereas c becomes independent of L for large L. We determine a, b, and c by fitting Σ^2 in the range $L \geqslant 1$. The calculated values are listed in Table I.

Next, to compare the results with the most popular and well-known statistics, we calculate the spectral rigidity Δ_3. For a level sequence with a constant average level spacing, the staircase function on the average follows a straight line. Thus it measures the fluctuations of the staircase function around a best fit straight line. We calculate $\Delta_3(L)$ [1] as

$$\Delta_3(L) = \left\langle \min_{a,b} \int_{E-\frac{L}{2}}^{E+\frac{L}{2}} [n(E) - a - bE]^2\, dE \right\rangle, \tag{22}$$

where $n(E)$ is determined from the density of states as in Eq. (20). In Fig. 3 we plot the $\langle\Delta_3(L)\rangle$ for the lowest 100 levels. For comparison we also plot the GOE results in the same figure, which shows that the spectrum is more correlated than GOE.

As pointed earlier, the time series analysis and the study of Fourier power spectrum of energy level sequence is the alternative and elegant way to understand the spectral fluctuation. To study the correlation and level repulsion between energy levels one can utilize the established analogy between the energy spectrum and discrete time series. The energy spectrum is considered as a discrete signal, and the fluctuations of the excitation energy are considered as discrete time series. The recent studies of statistical properties of random signals with logarithmic correlations attracted active interest in statistical mechanics and random matrix theory [40,41]. The δ_n statistics widely used in RMT to study correlation between consecutive level spacing is defined as

$$\delta_n = \sum_{i=1}^{n} (s_i - \langle s \rangle), \tag{23}$$

where the nearest-neighbor spacing is calculated as $s_i = \epsilon_{i+1} - \epsilon_i$, $i = 1,2,\ldots,n$. The average value of s_i is $\langle s \rangle = 1$, and δ_n represents the deviation of the $(n+1)$-th level from the mean value, i.e., the fluctuation of $(n+1)$-th excited state. Thus δ_n is similar to the time series, and n represents the discrete time [4–6,42]. Although there are some differences between δ_n and the actual time series [8], however, the analogy between an energy level spectrum and a time series is well established. Note that we calculate the energy levels for fixed interaction (fixed scattering length a_s) and fixed number of bosons. Thus in this regard it is well justified to study the robustness of δ_n statistics against changing the number of levels. In our earlier calculations, in this direction, focus has been made on a large set of energy levels, including both low- and high-level statistics. To find the crossover from Wigner to regular dynamics, we have already done the thorough calculation in Refs. [21,22] and determined the best fit window to the Wigner distribution comparing the level spacing distribution to Brody distribution, whereas our present study focuses only on the lowest 100 levels, which can be understood as a stringent test of our earlier works. However, for completeness we present the δ_n statistics for lowest 100 levels in Fig. 4. The observed antipersistent time series in Fig. 4 again confirms the presence of high-level correlation. Next, the Fourier power spectrum of δ_n gives the following results. It is verified that the Fourier power spectrum P_k^{δ} follows the power laws

$$P_k^{\delta} \propto \frac{1}{k^{\alpha}} \tag{24}$$

for both the fully chaotic and integrable systems. Thus the level fluctuation in chaotic quantum systems are characterized by $\frac{1}{f}$ noise, whereas that of integrable systems show $\frac{1}{f^2}$ noise [4–7].

In our earlier study in this direction we have observed that the system of interacting trapped bosons at zero temperature is a very complex system. The low-lying collective excitations

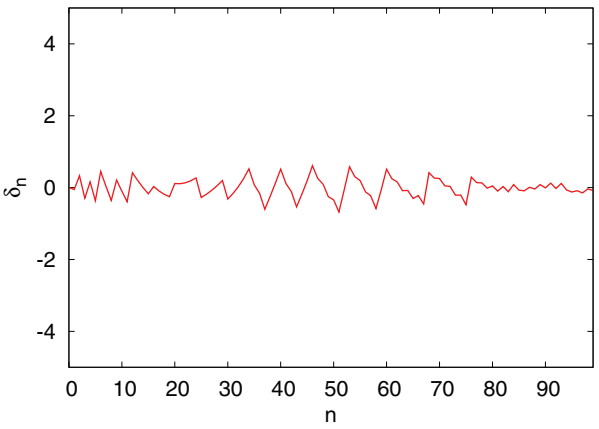

FIG. 4. (Color online) Red line is the plot of δ_n, numerically calculated against n for $N = 5000$ numbers of interacting trapped bosons and lowest 100 levels.

are strongly affected by the interatomic interaction when the high-lying excitations are of single-particle nature. We have studied the transition from collective to single-particle excitations and observed its immediate reflection in the study of level correlation. In our earlier study we have shown that the interacting trapped bosons is neither integrable nor chaotic; it shows a very complex distribution and $\frac{1}{f^\alpha}$ noise with $1 < \alpha < 2$. However, to get a deeper understanding of the power fluctuation properties we go beyond the study of the power spectrum. The power spectrum of δ_n is related only to the second-order correlation function and does not provide information on the correlation structure. Thus the purpose of our study is to explore the correlation structure and higher-order moments. We are especially interested in the qth-order height-height correlation function $[C_q(\tau)]$ for higher-order moments. $C_q(\tau)$ measures the moment of order q, i.e., the average qth power of the signal changes after a time delay τ. In the earlier study of qth-order height-height correlation function, the logarithmic correlation structure is found instead of multiscaling structure in classical random matrix ensembles [8,43]. Thus the interacting trapped bosons will be a very realistic quantum system to investigate whether the qth-order height-height correlation function exhibits the same properties.

Now, for a continuous time series $X(t)$, the qth-order height-height correlation function is given by [8]

$$C_q(\tau) = \langle |X(t) - X(t+\tau)|^q \rangle_t. \tag{25}$$

However, the discrete energy spectrum of quantum system is related to discrete time series. For a discrete and finite time series $X(n)$, $n = 1,2,\ldots,N$ the power spectrum is defined as [8]

$$P(\omega_k) = |\hat{X}(\omega_k)|^2, \tag{26}$$

while $\omega_k = \frac{2\pi k}{N}$ and $k = 1,2,\ldots,\frac{N}{2}$. Thus the discrete Fourier transform of the signal is

$$\hat{X}(\omega_k) = \frac{1}{\sqrt{N}} \sum_{n=1}^{N} X(n) \exp(-i\omega_k n). \tag{27}$$

For such discrete time series, the qth-order correlation function is defined as

$$C_q(n) = \langle |X(m) - X(m+n)|^q \rangle_m = \frac{1}{Q} \sum_{m=1}^{Q} |X(m) - X(m+n)|^q, \tag{28}$$

where Q is the number of points over which the moving average is taken [8]. For the calculation of qth-order correlation, we perform a twofold average, first, a moving average over each spectrum, and then the ensemble average over different members of the same ensemble, and thus

$$C_q(n) = \overline{\langle |\delta(p+n) - \delta(p)|^q \rangle_p}. \tag{29}$$

This dual average significantly reduces the statistical fluctuation especially for high values of q.

It is worth to note that $C_q(n)$ carries much information of the correlation structure of the time series. However, the second-order correlation function $C_2(n)$ is directly related to the power spectrum like Eq. (26) as [8]

$$C_2(\tau) = \frac{2}{\pi} \int_0^\infty d\omega P(\omega)[1 - \cos(\omega\tau)]. \tag{30}$$

For the finite and discrete time series the second-order momentum is given by [44]

$$C_2(n) = A_2 \ln n + B_2. \tag{31}$$

It was pointed out earlier that many natural phenomena that are characterized by time series with power spectra of form

$$P(\omega) \sim \frac{1}{\omega^\alpha} \quad (\alpha \geqslant 1) \tag{32}$$

show multiscaling behavior in the second-order correlation function, i.e.,

$$C_2(n) \sim n^{\alpha-1}. \tag{33}$$

However, for generic chaotic quantum systems showing $\frac{1}{f}$ conjecture $C_2(n)$ behaves logarithmically. For our present study, we first calculate the δ_n statistics for the trapped bosons with the same parameters used in the calculation of other correlation properties. We again concentrate on lowest 100 levels, which are highly correlated and exhibit GOE prediction. We calculate $C_2(n)$ for 5000 bosons and plot it in Fig. 5 as a function of $\ln n$. The results of GOE are also presented for comparison. We observe that for the whole range of n values, the calculated points fit very well with the law given by Eq. (31).

The values of A_2 and B_2 are obtained from least-squares fitting. The best fit numerical values of the coefficients are $A_2 = 0.1902$ and $B_2 = 0.2985$, which compare well with the GOE results of Refs. [8,44], i.e., $A_2 = 0.2026$ and $B_2 = 0.2753$.

In Fig. 6 we present the qth-order momentum $C_q(n)$ for wide intervals of q. For clarity the figures are divided in subpanels with different types of scales. It nicely demonstrates the correlation structure and the main trend of the correlation function through the whole interval of q. The upper subpanel (a) presents the double logarithmic scale. The calculated results for various q values fit well with

$$C_q(n) = (A_q \ln n + B_q)^{\frac{q}{2}}. \tag{34}$$

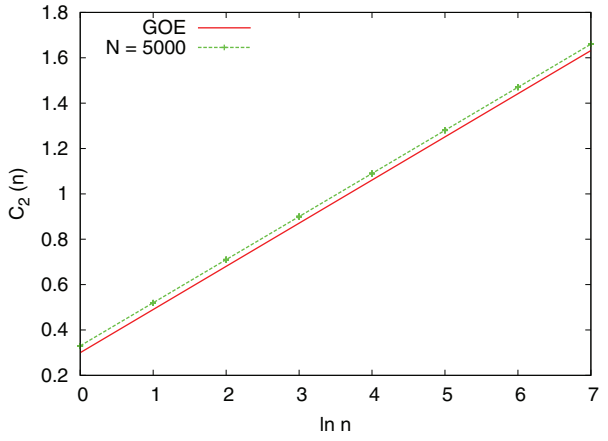

FIG. 5. (Color online) Blue points are the plots of numerically calculated values of $C_2(n)$ against $\ln n$ for the lowest 100 levels and $N = 5000$ numbers of interacting trapped bosons. The red line is the plot of same for GOE.

Solid lines represent the results of least-squares fit according to Eq. (34). The agreement between the numerical values

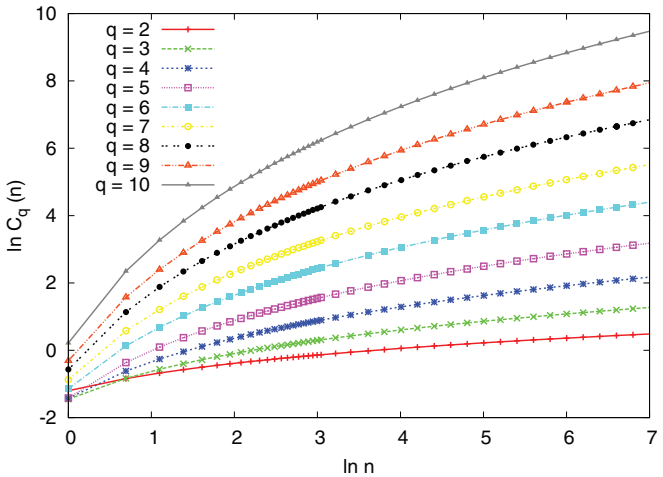

(a)

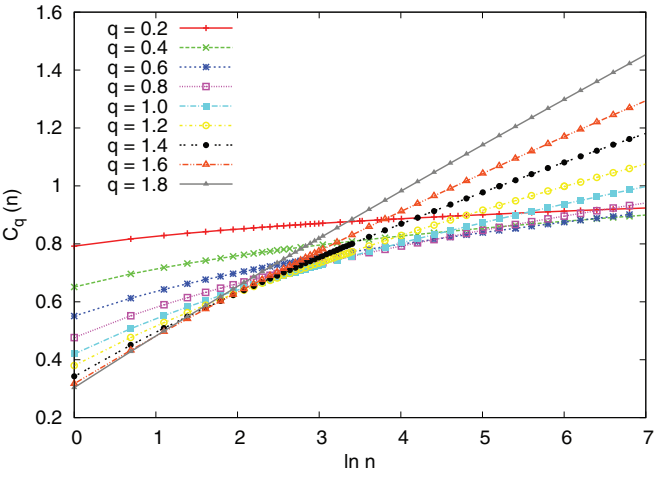

(b)

FIG. 6. (Color online) The plot of numerically calculated values of $\ln C_q$ (a) and $C_q(n)$ (b) against $\ln n$ of lowest 100 levels of ($N =$) 5000 numbers of interacting trapped bosons.

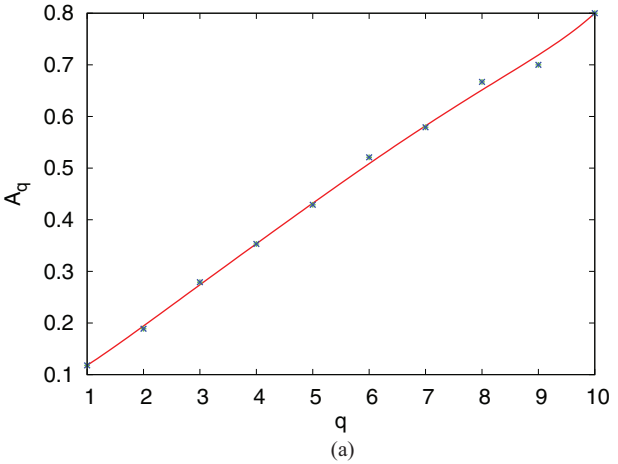

(a)

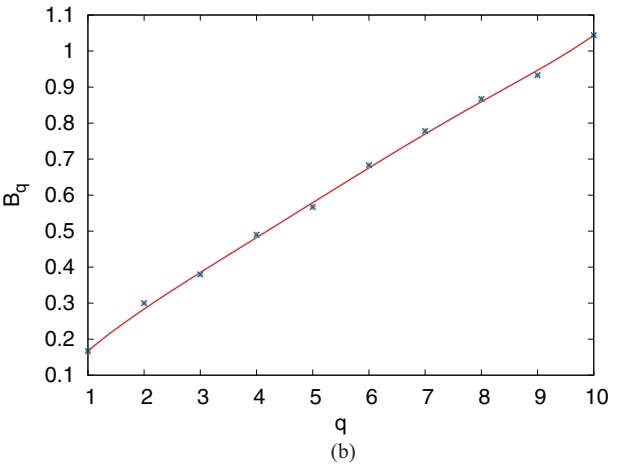

(b)

FIG. 7. (Color online) (*a*) Plot of A_q and (*b*) B_q against q; both for lowest 100 levels of $N = 5000$ numbers of interacting trapped bosons.

of $C_q(n)$ and the continuous curves is excellent. Although Eq. (34) is the generalization of Eq. (31) for $q = 2$, small discrepancies between the GOE prediction and the calculated results appear for very small values of n. It again supports our earlier findings that even for the lowest 100 levels although the system is highly correlated, the spectral distribution is not strictly Wigner. The interplay between the interatomic interaction and external trap plays an important role. Moreover the deviation from the GOE spectra reveals that the power spectrum does not show $\frac{1}{f}$ noise strictly even when the system is highly correlated and shows level repulsion. Here the higher order correlation function exhibits the logarithmic behavior like Eq. (34). We obtain the linear dependence of A_q and B_q in q. In order to characterize the correlation structure we calculate A_q and B_q for different q and plot in Fig. 7. It is seen that both functions increase with q, and their plots are more or less straight lines. In this work we obtain values of the elements for $1 \leqslant q \leqslant 10$. Beyond this interval larger dimensionalities and number of members of the matrix ensemble are needed [8].

IV. CONCLUSION

In the present study we introduce the two-level correlation properties and give precise measures of level repulsion and

long-range order in the spectra of interacting trapped bosons. We choose the spectra of ^{87}Rb atoms in the JILA trap and calculate the low-lying excitations by introducing a correlated many-body technique. In the present study we consider only the lowest hundred levels, which are highly correlated, and experimental results show that these low-lying levels are of a collective nature. It is emphasized that an interacting trapped bosonic system is highly complicated due to the presence of two energy scales, as stated earlier. However, the low-lying modes of excitations are highly influenced by the interatomic interaction. Our calculated values of two-level correlation measures show the signature of chaos in the energy spectrum. Next we use the formal analogy between energy level spectra and time series and calculate the correlation structure in the spectra. We calculate the qth-order correlation function $C_q(n)$ for wide range of q values $0 < q \leqslant 10$ using a twofold average. This ensures high accuracy for the higher-order correlation structure. We observe that the second-order correlation function $C_2(n)$ maintains the linear behavior with $\ln n$, which supports the GOE results of random matrix ensembles.

Thus our present calculation nicely demonstrates that the various statistical properties of such a realistic system support the earlier findings of random matrix theory and provide the stringent test of Bohigas-Giannoni-Schmit conjecture.

ACKNOWLEDGMENT

This work is supported by the Department of Atomic Energy (DAE), government of India, through Grant No. 2009/37/23/BRNS/1903.

[1] O. Bohigas, in *Random Matrix Theories and Chaotic Dynamics*, Les Houches, Session LII (1989), Chaos and Quantum Physics, Course 2, edited by M.-J. Giannoni *et al*. (Elsevier Science Publishers, North-Holland, 1991), pp. 87–199.
[2] H.-J. Stöckmann, *Quantum Chaos* (Cambridge University Press, Cambridge, 1999).
[3] F. Haake, *Quantum Signatures of Chaos* (Springer, New York, 2010).
[4] A. Relaño, J. M. G. Gómez, R. A. Molina, and J. Retamosa, and E. Faleiro, Phys. Rev. Lett. **89**, 244102 (2002).
[5] A. Relaño, J. Retamosa, E. Faleiro, R. A. Molina, and A. P. Zuker, Phys. Rev. E **73**, 026204 (2006).
[6] J. M. G. Gómez, A. Relaño, J. Retamosa, E. Faleiro, L. Salasnich, M. Vranicar, and M. Robnik, Phys. Rev. Lett. **94**, 084101 (2005).
[7] A. Relaño, Phys. Rev. Lett. **100**, 224101 (2008).
[8] A. Relaño, J. Retamosa, E. Faleiro, and J. M. G. Gómez, Phys. Rev. E **72**, 066219 (2005).
[9] G. Casati, F. Valz-Gris, and I. Guarneri, Lett. Nuovo Cimento Soc. Ital. Fis. **28**, 279 (1980).
[10] T. H. Seligman, J. J. M. Verbaarschot, and M. R. Zirnbauer, Phys. Rev. Lett. **53**, 215 (1984).
[11] T. Zimmermann, H.-D. Meyer, H. Köppel, and L. S. Cederbaum, Phys. Rev. A **33**, 4334 (1986).
[12] G. Tanner, K. Richter, and J.-M. Rost, Rev. Mod. Phys. **72**, 497 (2000).
[13] J. Sakhr and N. D. Whelan, Phys. Rev. A **62**, 042109 (2000).
[14] T. A. Brody *et al*., Rev. Mod. Phys. **53**, 385 (1981).
[15] V. K. B. Kota, Phys. Rep. **347**, 223 (2001).
[16] J. M. G. Gómez, K. Kar, V. K. B. Kota, R. A. Molina, A. Relaño, and J. Retamosa, Phys. Rep. **499**, 103 (2011).
[17] L. Muñoz, E. Faleiro, and R. A. Molina, A. Relaño, and J. Retamosa, Phys. Rev. E **73**, 036202 (2006).
[18] R. J. Leclair, R. U. Haq, V. K. B. Kota, and N. D. Chavda, Phys. Lett. A **372**, 4373 (2008).
[19] N. D. Chavda, V. Potbhare, and V. K. B. Kota, Phys. Lett. A **311**, 331 (2003).
[20] M. Vyas, V. K. B. Kota, N. D. Chavda, and V. Potbhare, J. Phys. A: Math. Theor. **45**, 265203 (2012).
[21] K. Roy, B. Chakrabarti, A. Biswas, V. K. B. Kota, and S. K. Haldar, Phys. Rev. E **85**, 061119 (2012).
[22] B. Chakrabarti, A. Biswas, V. K. B. Kota, K. Roy, and S. K. Haldar, Phys. Rev. A **86**, 013637 (2012).
[23] D. S. Jin, J. R. Ensher, M. R. Matthews, C. E. Wieman, and E. A. Cornell, Phys. Rev. Lett. **77**, 420 (1996).
[24] F. Dalfovo, S. Giorgini, M. Guilleumas, L. Pitaevskii, and S. Stringari, Phys. Rev. A **56**, 3840 (1997).
[25] O. Bohigas, R. U. Haq, and A. Pandey, Phys. Rev. Lett. **54**, 1645 (1985).
[26] T. K. Das and B. Chakrabarti, Phys. Rev. A **70**, 063601 (2004).
[27] T. K. Das, S. Canuto, A. Kundu, and B. Chakrabarti, Phys. Rev. A **75**, 042705 (2007).
[28] T. K. Das, A. Kundu, S. Canuto, and B. Chakrabarti, Phys. Lett. A **373**, 258 (2009).
[29] F. Dalfovo, S. Giorgini, L. P. Pitaevskii, and S. Stringari, Rev. Mod. Phys. **71**, 463 (1999).
[30] C. J. Pethick and H. Smith, *Bose-Einstein Condensation in Dilute Gases* (Cambridge University Press, Cambridge, 2001).
[31] J. L. Ballot and M. Fabre de la Ripelle, Ann. Phys. (N.Y.) **127**, 62 (1980).
[32] B. D. Esry and C. H. Greene, Phys. Rev. A **60**, 1451 (1999).
[33] M. Fabre de la Ripelle, Few Body Syst. **1**, 181 (1986).
[34] M. H. Anderson *et al*., Science **269**, 198 (1995).
[35] M. Abramowitz and I. A. Stegun, *Handbook of Mathematical Functions* (Dover Publications, New York, 1972), p. 773.
[36] A. Kundu, B. Chakrabarti, T. K. Das, and S. Canuto, J. Phys. B: At. Mol. Opt. Phys. **40**, 2225 (2007).
[37] T. K. Das, H. T. Coelho, and M. Fabre de la Ripelle, Phys. Rev. C **26**, 2281 (1982).
[38] A. Biswas and T. K. Das, J. Phys. B **41**, 231001 (2008).
[39] B. Chakrabarti, T. K. Das, and P. K. Debnath, J. Low Temp. Phys. **157**, 527 (2009).
[40] Y. V. Fyodorov, G. A. Hiary, and J. P. Keating Phys. Rev. Lett. **108**, 170601 (2012).
[41] Y. V. Fyodorov, P. Le Doussal, and A. Rosso, J. Stat. Phys. **149**, 8982 (2012).
[42] E. Faleiro, J. M. G. Gómez, R. A. Molina, L. Muñoz, A. Relaño, and J. Retamosa, Phys. Rev. Lett. **93**, 244101 (2004).
[43] F. N. Hooge and P. A. Bobbert, Physica B **239**, 223 (1997).
[44] O. Bohigas, P. Leboeuf, and M. J. Sánchez, Physica D **131**, 186 (1999).